XXXX

Design and Analysis of a 170 m Span Network Hanger Tied-Arch Bridge

Dongwei Luo

[1] Shanghai Municipal Engineering Design Institute (Group) Co., Ltd., Shanghai 200092, China.
* Correspondence: 425756691@qq.com

Abstract: Based on the 170 m span network hanger tied-arch bridge of the Guangming Road Guohe Bridge in Bozhou city, structural design and mechanical characteristic analysis are carried out in this study to address the problems associated with traditional vertical hangers in medium-to-large span tied-arch bridges, namely, their susceptibility to slackness, insufficient stiffness, and inadequate stability. The main bridge is a single-span 170 m network hanger tied-arch bridge. The main girder is a double-box steel–concrete composite girder, and the arch rib is an octagonal steel box section without transverse bracing. The hangers are arranged in a crossed network pattern, and the substructure adopts a friction pendulum seismic isolation system. Static, stability, and seismic calculations are performed using the finite element method. The results show that the network hangers can significantly improve the internal force distribution of the main girder and arch rib, reducing both bending moments and deflections. The structural stiffness and stability satisfy the code requirements. The seismic isolation design effectively reduces the seismic response of the piers, and the seismic performance meets the relevant standards. This bridge type demonstrates good technical feasibility and economic rationality for wide urban bridges with spans of 150–200 m and can serve as a reference for similar projects.

Keywords: network hanger; tied-arch bridge; steel-concrete composite girder; structural design; mechanical analysis; seismic isolation

Design and Construction

Citation: Dongwei Luo. Design and Analysis of a 170 m Span Network Hanger Tied-Arch Bridge[J]. Prestress Technology, DOI:10.59238/j.pt.XXXX.XX.001.
Published: XX/XX/XXXX

Publisher's Note: Prestress technology stays neutral with regard to jurisdictional claims in published maps and institutional affiliations.

1 Introduction

Tied-arch bridges combine the load-bearing characteristics of an arch and a girder. Compared with traditional arch bridges, the use of a tie to resist horizontal thrust from the arch rib effectively reduces the bearing capacity required for the foundation. This bridge type has been widely used in highways, railways, and other transportation infrastructures and is a preferred option for crossing rivers and valleys. Most traditional tied-arch bridges adopt vertical hangers, which have simple structural behavior, are constructed by mature techniques and are highly suitable for small- and medium-span bridges. However, with increasing traffic demand, the required bridge span has increased. When the span reaches 150 m, the limitations of vertical-hanger tied-arch bridges become evident. Under asymmetric loads, the vertical hangers near the arch foot on the unloaded side are prone to slackness and loss of effectiveness. This leads to larger bending moments and vertical deflections in the arch rib and the tie girder, requiring larger member sections to meet the load-bearing requirements. Consequently, both material consumption and construction cost increase, and structural aesthetics are compromised. Moreover, the improvement in structural stiffness and stability is limited, which restricts the application of such bridges in long spans.

Given this background, network hanger tied-arch bridges have emerged. This bridge type was proposed by Professor Per Tveit of Norway in 1955, and its core

feature is that the hangers are arranged to intersect at least twice. Compared with traditional vertical hangers, network hangers can optimize the internal force distribution of the structure, reduce the bending moment amplitudes in the arch rib and the tie girder, and make the internal forces more uniform. As a result, slender members can be used to reduce material consumption, achieving both economy and aesthetics. Moreover, structural stiffness and stability are significantly improved, vertical deflections are reduced, and mechanical performance under asymmetric loads is enhanced [1-5]. Although some network hanger tied-arch bridges have been constructed both in China and abroad, the design parameters and mechanical characteristics of such bridges with medium-to-large spans of 150–200 m still need further investigation. Therefore, in this study, the main bridge of the Guangming Road Guohe Bridge in Bozhou city is taken as an engineering example to present the design and analysis of a 170 m span network hanger tied-arch bridge and provide a reference for future similar projects.

2 Project Overview

The Guangming Road Guohe Bridge in Bozhou city is a key node of the "one ring, two horizontals, two verticals" expressway network in the urban area of Bozhou, crossing the Guohe River channel. The planned navigation class of the river at the bridge site is Grade IV. In accordance with the relevant navigation design standards, the minimum vertical navigation clearance should not be less than 7 m, and the minimum horizontal navigation clearance should not be less than 105 m. The angle between the normal direction of the bridge axis and the water flow direction is approximately 5°. Considering the layout of the pier protection facilities and the width of the turbulence effects, the main span of the bridge should not be less than 135 m. The total width of the river channel at the bridge site is approximately 320 m, of which the main channel width is approximately 143 m. According to the flood discharge safety requirements of the river channel, the main channel should preferably be crossed by a single span. Considering the occupation of flood discharge space by the substructure dimensions, the main span needs to be further increased to no less than 170 m. When the two core requirements of navigation and flood discharge are combined, the main bridge is designed with a 170 m main span. In accordance with regional transportation planning, the bridge deck is arranged with eight lanes in both directions plus slow lanes on both sides. The design standard follows the relevant codes for urban expressways, and the vehicle load grade adopted is Urban Class-A. The seismic fortification intensity of the bridge site area is VII, with a corresponding peak ground acceleration of 0.10 g.

3 Overall Design

For a bridge with a main span of 170 m, the feasible bridge types mainly include cable-stayed bridges, self-anchored suspension bridges, and tied-arch bridges. From the perspective of the side-to-main span ratio, adopting a cable-stayed or self-anchored suspension bridge would inevitably increase the construction scale, engineering cost, and difficulty of construction of the main bridge. In contrast, the tied-arch bridge exhibits excellent economic efficiency for a span of 170 m. Moreover, it is externally statically determinate, which effectively accommodates the adverse effects of the soft soil foundation in the Bozhou area. Therefore, the tied-arch bridge scheme presents significant technical and economic advantages for the main bridge of this project.

The tied-arch bridge is a composite system bridge, where the overall load-bearing behavior is jointly provided by the arch rib, the tie girder, and the hangers, forming an organic whole through a rational force transmission path.

 https://doi.org/10.59238/j.pt.XXXX.XX.001

Among these components, the hangers serve as the core force-transmitting members between the arch rib and the tie girder, and their arrangement significantly affects the overall mechanical performance of the bridge. When the hangers are inclined in two directions and intersect at least twice, forming a network hanger system, the mechanical behavior of this type of tied-arch bridge resembles that of a truss structure: the arch rib acts as the top chord of the truss, primarily under compression; the tie girder acts as the bottom chord, mainly resisting tension and bending moments; and the hangers act as the web members, primarily under tension. Compared with vertical hangers, the inclined arrangement of the hangers significantly expands the range over which the deck loads are transmitted to the arch rib, thereby reducing the bending moments in the tie girder and the arch rib as well as the structural deformations and increasing the overall load-carrying capacity of the structure. In addition, because the network hangers form a mesh-like pattern within the plane of the arch rib, the in-plane stability of the arch rib is substantially improved compared with that of a tied-arch bridge with vertical hangers.

Considering various factors, such as the geological conditions at the bridge site, navigation requirements, flood control standards, and structural performance, the main bridge of the Guangming Road Guohe Bridge in Bozhou city was ultimately designed as a single-span 170 m network hanger tied-arch bridge, as shown in Figure 1. The total deck width is 54.2 m, with the deck accommodating motor vehicle lanes, nonmotorized vehicle lanes, and sidewalks, as shown in Figure 2.

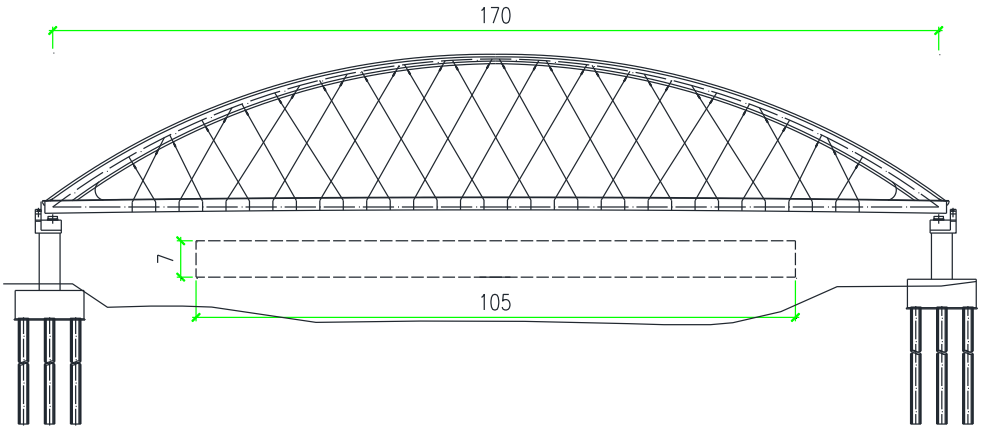

Figure 1 Elevation layout of the main bridge of the Guangming Road Guohe Bridge (unit: m)

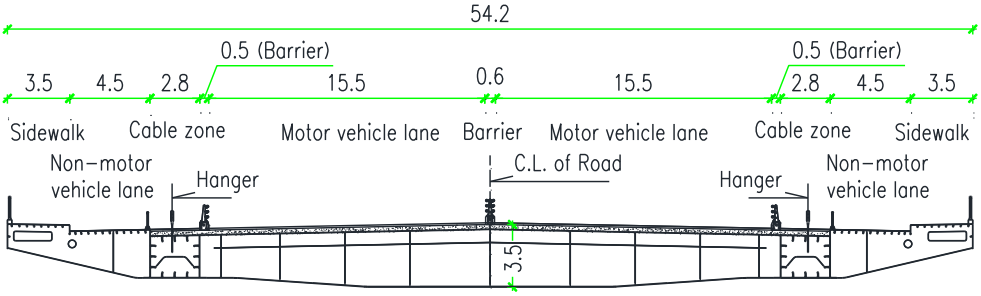

Figure 2 Standard cross-section layout of the main bridge of the Guangming Road Guohe Bridge (unit: m)

4 Structural Design

4.1 Arch Rib Design

The arch axis is a key factor influencing the distribution and magnitude of internal forces in the arch rib. In general, the pressure line under dead load should

be kept in alignment with the arch axis as much as possible. For network hanger arch bridges, after the deck system loads are transferred to the network hangers, the load on the arch rib becomes closer to a radial load. Therefore, a circular arc is adopted as the arch axis of the arch rib in this bridge.

Given the considerable deck width of this project, two or three arch ribs can be arranged transversely. Three arch ribs reduce the size of each rib but significantly increase the cross-sectional width and impair the visual effect of the bridge deck. Although they are slightly larger in terms of individual section dimensions, two arch ribs reduce the construction workload and provide a wider field of vision for traffic. They have advantages in terms of both economy and aesthetics. Moreover, owing to the limited deck width, an inward-inclined arrangement is not feasible. Consequently, two parallel arch ribs are adopted.

The rise-to-span ratio of the arch rib is a core characteristic parameter in arch bridge design. It directly determines the horizontal tension in the tie girder and the internal force distribution in the arch rib and significantly influences the overall aesthetic appearance of the bridge. A rise-to-span ratio that is too small considerably increases the horizontal tension in the tie girder. Conversely, while effectively reducing the horizontal forces in the tie girder, an excessively large rise-to-span ratio greatly increases the difficulty of prefabrication, assembly, and on-site erection of the arch ribs and also weakens the overall aesthetic harmony of the bridge. A review of existing steel arch bridge projects reveals that a reasonable rise-to-span ratio is typically in the range of 1/4 to 1/6. On the basis of a comprehensive comparison considering the aesthetic requirements and structural loading conditions of this project, the arch rib rise is set to 28.5 m, corresponding to a rise-to-span ratio of 1/5.97.

In accordance with aesthetic requirements, an octagonal steel box section with a width of 2.8 m is adopted for the arch rib. The section height at the crown is 1.8 m, and it linearly increases along the arch axis to 3.5 m at the arch springing point. The number of web stiffeners increases from one at the crown to three at the springing point, as shown in Figure 3. The thicknesses of the top plate, bottom plate, web plates, and longitudinal stiffeners of the arch rib range from 36 mm to 55 mm. Ordinary diaphragms are arranged at approximately 3.5 m intervals along the arch axis, with a thickness of 20 mm; at the hanger attachment points, additional diaphragms with a thickness of 45 mm are provided. The ordinary diaphragms are set perpendicular to the arch axis. The arch-to-girder connection zone is subjected to complex forces. In this 16 m long segment, Q420qD steel is used, whereas Q345qD steel is used for the remaining parts of the arch rib.

4.2 Main Girder Design

The main girder types suitable for network hanger tied-arch bridges include mainly concrete girders, steel girders, and steel-concrete composite girders. Owing to its large self-weight, a concrete girder leads to a corresponding increase in the size of the arch rib structure, making the out-of-plane stability of the arch rib a controlling factor. A steel girder offers advantages such as easily assured construction quality and rapid on-site erection. However, the deck pavement cost is high, and the maintenance and repair workload are large. Moreover, heavy vehicles seriously challenge the fatigue performance of steel decks. In contrast, the concrete deck slab of a steel-concrete composite girder can effectively solve the fatigue problems caused by the low deck stiffness of a steel girder while also achieving good integration of the main structural system and the pavement. Therefore, a double-box steel-concrete composite girder is adopted as the main girder of this bridge. The steel part is a double-box longitudinal and transverse girder grillage system, and the concrete deck slabs are placed within the motor vehicle lane. The steel girder con-

 https://doi.org/10.59238/j.pt.XXXX.XX.001

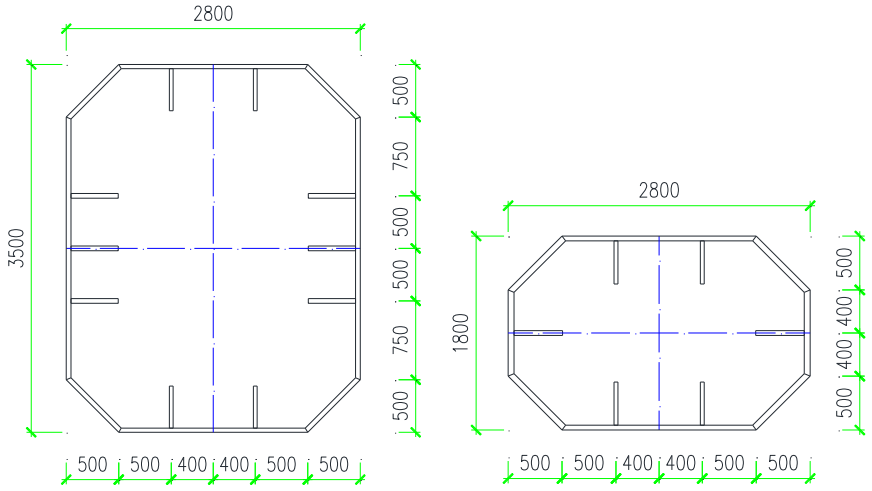

a) Springing section

b) Crown section

Figure 3 Cross sections of the arch rib (unit: mm)

sists of standard segments and arch-to-girder connection segments. The steel girder in the standard segments is composed of Q345qD steel. The arch-to-girder connection segment is 16 m long. With the exception of the webs of the main longitudinal girders and the stiffeners under the bearings, which are composed of the same Q420qD steel used for the arch rib, all the other plates are composed of Q345qD steel.

4.2.1 Standard Segment of the Steel Girder

The standard segment of the steel girder is a double-longitudinal-girder grillage system consisting of main longitudinal girders, standard cross girders, cantilever arms, and secondary longitudinal girders. The steel girder depth at the structural centerline is 3.24 m, and a standard cross girder is arranged every 4.5 m along the bridge longitudinal direction. To accommodate the vertical arch rib configuration, the double longitudinal girders have rectangular sections, with their webs aligned with those of the arch rib. The depth of the main longitudinal girder at its center is 2.386 m, and its width is 2.8 m. The internal diaphragms in the main longitudinal girder are of two types: ordinary diaphragms (16 mm thick) and hanger point diaphragms (32 mm thick). The ordinary diaphragms are arranged vertically and aligned with the webs of the cross girders. The hanger point diaphragms are placed between two standard cross girders and are arranged with an inclination consistent with the angle of the hangers.

Owing to the large deck width and the transverse load transfer requirements, the standard cross girders are designed as solid-web structures with I-shaped variable-depth sections. The section depth ranges from 2.414 m to 3.240 m. Both the top and bottom flange widths are 600 mm. The top flange thickness is 20 mm, and the bottom flange thickness is 24, 32, or 36 mm. The web thickness is 16 mm at the mid-span transversely and increases to 20 mm near the supports of the main longitudinal girders.

The standard cantilever arms include a nonmotorized vehicle lane and a sidewalk, both of which are orthotropic steel deck structures. The deck plate thickness is 14 mm over the 4.5 m width of the nonmotorized vehicle lane and 12 mm over the 3.5 m width of the sidewalk.

The secondary longitudinal girders in the standard segment consist of three cross-girder secondary longitudinal girders placed between the cross girders. They have I-shaped sections with a depth of 500 mm, a top flange width of 500 mm, a

bottom flange width of 300 mm, top and bottom flange thicknesses of 16 mm, and a web thickness of 12 mm. The standard cross section of the main girder is shown in Figure 4.

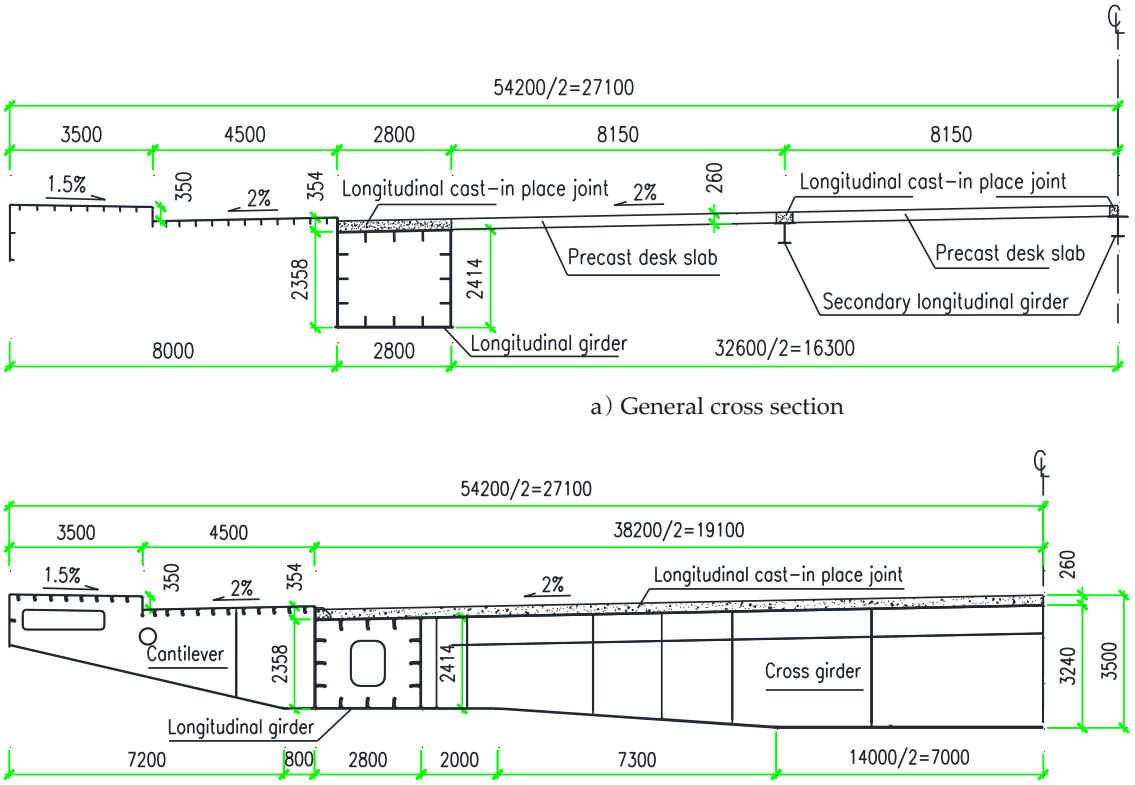

a) General cross section

b) Diaphragm cross section

Figure 4 Standard cross section of the main girder (unit: mm)

4.2.2 Arch-to-Girder Connecting Segment of the Steel Girder

In the segment connecting the arch to the girder, the webs of the main longitudinal girder and the arch rib share a common plane. The web thickness is increased to 45 mm to match that of the arch rib web. The top plate thickness is 36 mm, and the bottom plate thickness is 32 mm.

The transverse global stability of a tied-arch bridge is related to the stiffness of the end cross girders. Since the two arch ribs of this bridge have no transverse bracing, the stiffness of the end cross girders must be increased in the design. In this design, the cross-sectional form of the end cross girder is changed from a conventional I-shaped section to a box section to increase the structural stiffness. The box-shaped end cross girder has a longitudinal (bridge direction) width of 6.445 m, a bottom plate thickness of 20 mm, and a top plate thickness of 16 mm. Three webs are provided, each with a thickness of 16 mm. The end cross girder is equipped with 11 solid-web diaphragms with a thickness of 14 mm spaced at intervals of 2.7 m to 2.75 m.

The details of the arch-to-girder connection are shown in Figure 5.

4.2.3 Concrete Deck Slab

To prevent fatigue cracking in the steel deck under vehicle loading, a 260 mm thick C50 concrete deck slab is adopted within the motor vehicle lane. The deck slab is prefabricated in segments and connected by cast-in-place wet joints. Transversely, it is divided into four prefabricated panels with five longitudinal cast-in-place joints. At the wet joints, the concrete deck slab and the steel girder are connected by stud shear connectors welded to the top plate of the steel girder. The cast-in-place wet joints are prepared using C50 micro-expansive fiber-reinforced

 https://doi.org/10.59238/j.pt.XXXX.XX.001

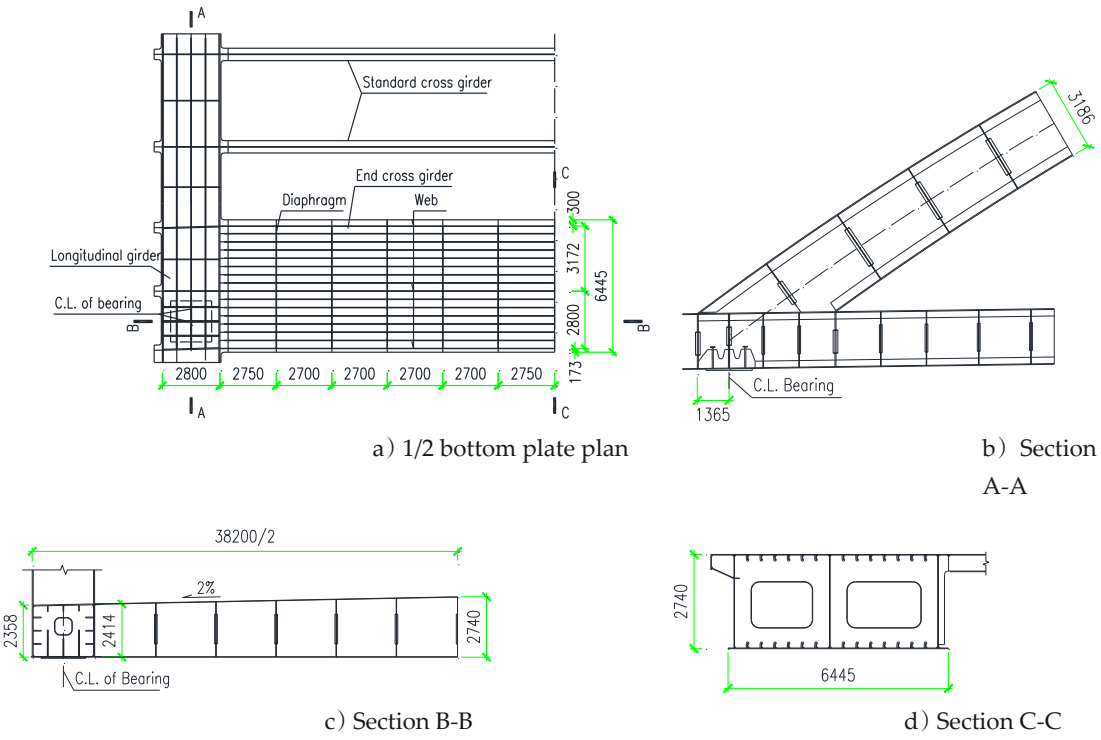

a) 1/2 bottom plate plan

b) Section A-A

c) Section B-B

d) Section C-C

Figure 5 Details of the arch-to-girder connection (unit: mm)

concrete. The longitudinal reinforcement of the deck slab is as follows: in the vehicular lane area, the top layer and bottom layer have dimensions of Φ25@120 mm and Φ28@120 mm, respectively; at the main longitudinal girder, the top layer and bottom layer have dimensions of Φ25@120 mm and Φ25@120 mm, respectively; and at the arch springing, both the top and bottom layers have dimensions of Φ28@120 mm. The transverse reinforcement of the deck slab is as follows: for the edge panels, both the top and bottom layers have dimensions of Φ20@120 mm; for the middle panels, both the top and bottom layers have dimensions of Φ16@120 mm.

4.3 Hanger Design

In domestic and international network hanger tied-arch bridges, the hanger spacing along the girder is generally uniform. The spacing value is related to the deck system, arch rib forces, and construction method and is determined comprehensively considering the hanger forces, structural detailing requirements, economy, and aesthetics. It is usually an integer multiple of the diaphragm spacing. In this project, the main girder is a double-box steel-concrete composite girder with a diaphragm spacing of 4.5 m. The optimal hanger spacings are 4.5 m and 9.0 m. Considering the large deck width of this project, a larger hanger spacing would increase the hanger size and the difficulty of the hanger-to-arch and hanger-to-girder anchorage details. Moreover, a denser spacing allows for better use of the mechanical advantages of the network hanger tied-arch system. Therefore, the hanger spacing is set to 4.5 m, which is consistent with the diaphragm spacing.

Network hangers generally have a constant inclination angle. If the inclination angle is too small, the horizontal force component becomes excessively large while the vertical component is insufficient, which is unfavorable for structural behavior. If the inclination angle is too large, the vertical force component becomes excessively large while the horizontal component is insufficient; thus, the mechanical characteristics of the network hanger system are not exploited. Therefore, the inclination angle of network hangers is usually controlled within the range of 45° to 75° [6]. Considering aesthetic effects, the hanger inclination angle in this project is 60°.

A total of 64 hangers are used in this bridge. The hanger cable bodies are 27-φS15.2 mm and 31-φS15.2 mm epoxy-coated steel strands, with a standard tensile strength of $f_{ptk} = 1,860$ MPa. The fatigue performance of the hangers should satisfy the following requirements: with an upper stress limit of $0.45f_{ptk}$ and a stress of 200 MPa, no fracture should occur after 2 million cycles of loading.

Owing to the inclined arrangement, installation and tensioning are more complex for the hangers than for the vertical hangers. Therefore, the connections at both the girder end and the arch end of the hangers must be as simple as possible. In this bridge, pinned clevis joints are adopted at both ends and are made of Q345qD steel, and tensioning is performed at the girder end. A schematic view of the hanger is shown in Figure 6.

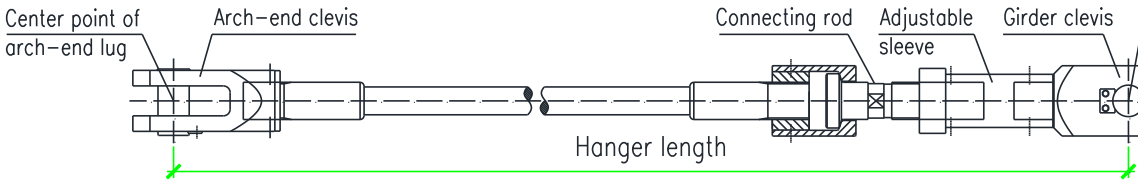

Figure 6 Schematic view of a hanger

At the girder end, the hanger anchorage adopts a pinned anchor plate in the longitudinal direction, as shown in Figure 7. The standard thickness of the anchor plate is 45 mm, which is increased to 100 mm at the pin hole of the lug. Two circular reinforcing plates of 30 mm thickness are added at the pin hole, and the pin hole diameter is 190 mm. The anchor plate passes through a slot in the top plate and is inserted into a notch in the hanger diaphragm located inside the main longitudinal girder.

At the arch end, a pinned anchor plate is adopted for the hanger anchorage in the transverse direction and is arranged orthogonally to the anchor plate at the girder end. This configuration allows the hanger to better accommodate rotational deformations in both the longitudinal and transverse directions [7]. The remaining details are the same as those at the girder end. The inclined hanger diaphragm protrudes through the bottom plate of the arch rib and shares a common plane with the anchor plate, as shown in Figure 8.

4.4 Substructure Design

The bridge piers are double-column piers with uniform circular-ended cross sections. The cross-sectional dimensions are 4 m (longitudinal direction) × 6 m (transverse direction), and the radius of the circular ends is 3 m. The pile caps have a separated pointed-oval shape, and 2 m diameter bored piles are used for the foundations. The pile tips are embedded in the grayish–yellow to brownish–yellow silty clay layer as the load-bearing stratum. The piles are designed as friction piles with a length of 75 m. The layout of the substructure is shown in Figure 9.

The substructure design is governed by seismic loading conditions. For the main bridge of this project, a simply supported structural system is adopted. The pier heights range from 13 m to 18 m, and the ratio of the pier height to the section depth is small, resulting in an insufficient inherent ductility reserve of the structure. Considering the structural characteristics and overall mass distribution, a seismic isolation design is suitable for this bridge [8-9]. A total of four friction pendulum seismic isolation bearings are installed on the tops of the piers. To ensure the structural capacity of the bridge and its ability to resist deformation under normal service conditions, shear pins are added to the longitudinal bearing of one pier and the transverse bearings on one side of the two piers. The horizontal load-carrying capacity of these pins is set to 10% of the vertical bearing capacity of the bearing. When the earthquake-induced horizontal shear force exceeds the shear

 https://doi.org/10.59238/j.pt.XXXX.XX.001

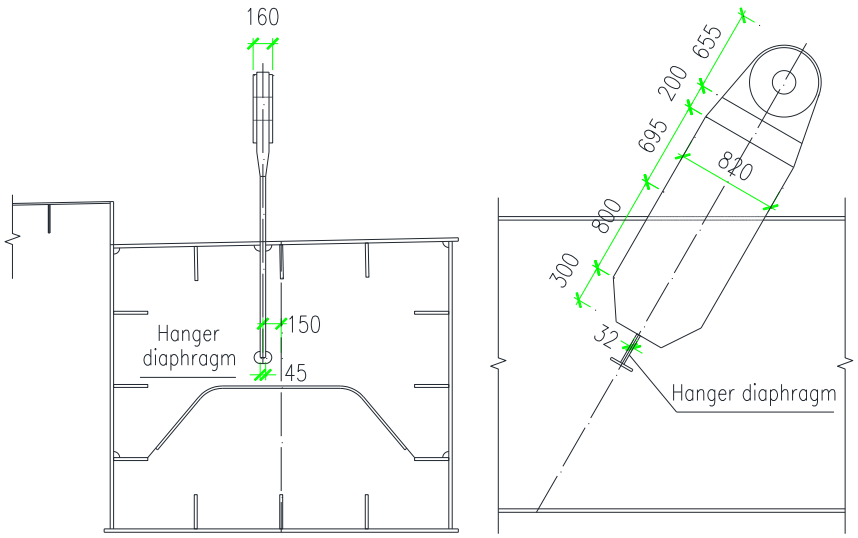

a) Transverse direction

b) Longitudinal direction

Figure 7 Anchorage detail of a hanger at the girder end (unit: mm)

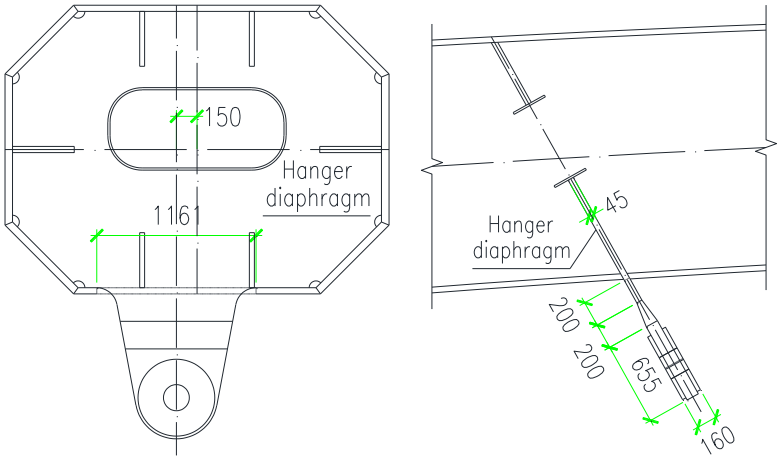

a) Transverse direction

b) Longitudinal direction

Figure 8 Anchorage detail of a hanger at the arch end (unit: mm)

capacity of the pin, the shear pin fractures and unlocks. All the friction pendulum bearings on the bridge subsequently become activated and dissipate seismic energy effectively through their own hysteretic deformation.

4.5 Construction Method Design

The main bridge of this project is constructed with a conventional method, with the girder erected before the arch using minimum scaffolding. The steel struc-

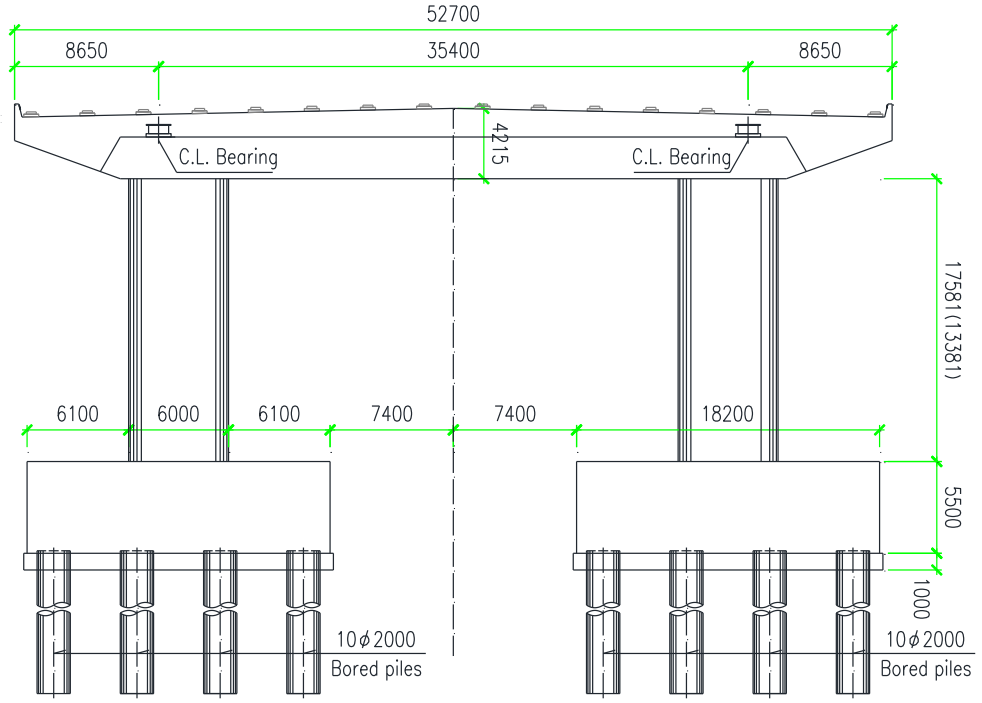

Figure 9 Layout of the substructure（unit：mm）

ture of the main bridge is prefabricated in segments in the factory and transported to the site by road. The on-site construction procedure includes erecting a small number of scaffolds in the river to hoist and assemble the steel girder segments; installing the arch rib segments and precast deck slabs on the girder, followed by tensioning of the hangers; and, finally, removing the steel girder scaffolds and casting the wet joints of the deck slab.

5 Structural Calculation and Analysis

5.1 Static Analysis

5.1.1 Global Analysis

A spatial finite element model of the entire bridge was established using finite element analysis software. The main girder was modeled using a double-main-girder approach. The main longitudinal girders, arch rib, pier columns, cap beams, and pile caps were simulated with beam elements. The hangers were simulated with truss elements. The steel deck was simulated with shell elements. Since the concrete deck slab of an arch bridge under serviceability limit conditions is subjected to small eccentric tension and, therefore, cracks, the concrete deck slab was considered cracked in the global analysis, meaning that only the reinforcement in the concrete slab was considered to participate in load carrying. For modeling convenience, the reinforcement was simulated with shell elements through stiffness equivalence. The steel superstructure was constructed with scaffolding support. The precast concrete deck slabs were installed before hanger tensioning and before the main girder was lowered off the scaffolding. The wet joints of the concrete deck slab were cast after the main girder was lowered off the scaffolding. This ensures that the self-weight of the precast concrete slabs is carried solely by the steel structure of the main girder while the secondary dead loads and subsequent live loads are carried by both the steel structure and the concrete deck slab, thereby making full use of the tensile capacity of the steel structure. The following load cases were considered in the analysis: dead load, live load, temperature load, wind load, foundation settlement, shrinkage and creep, and cable loss. The spatial finite element model is shown in Figure 10.

 https://doi.org/10.59238/j.pt.XXXX.XX.001

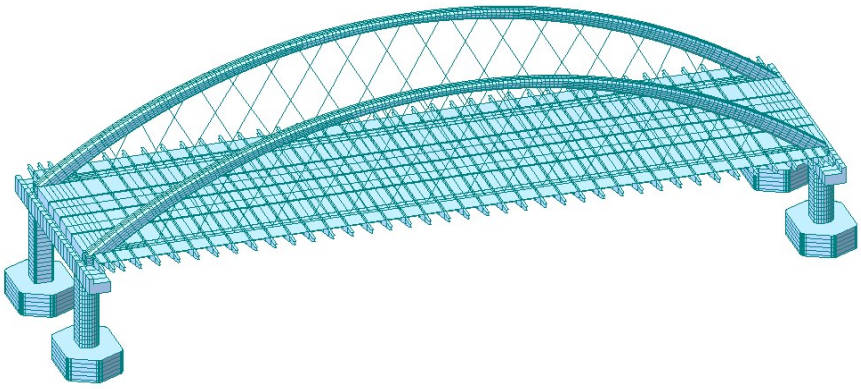

Figure 10 Spatial finite element model of the bridge

(1) Analysis of the Main Girder

Under a live load, the maximum vertical deflection of the main girder is 42 mm (see Figure 11), corresponding to a deflection-to-span ratio of 1/4, 047, which is far smaller than the allowable value of 1/800 specified in the code. This finding indicates that the network hanger tied-arch bridge features high vertical stiffness and small live-load deflection.

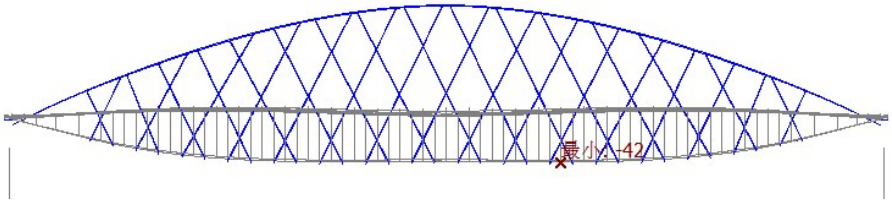

Figure 11 Vertical deflection of the main girder under live load（unit：mm）

Under the most unfavorable load combination for load-carrying capacity, the total stress envelope and the axial stress envelope of the main longitudinal girder are shown in Figures 12 and 13, respectively. The maximum stress in the main longitudinal girder is 249 MPa, which is less than the allowable value of 275 MPa specified in the code. The stresses and their proportions at typical locations of the main longitudinal girder are presented in Table 1. The calculation results reveal that, except for the region without hangers near the arch springing, the ratio of bending stress to total stress in the main girder is less than 20% at all locations. This finding indicates that the network hanger arrangement is capable of reducing bending moments in the main girder.

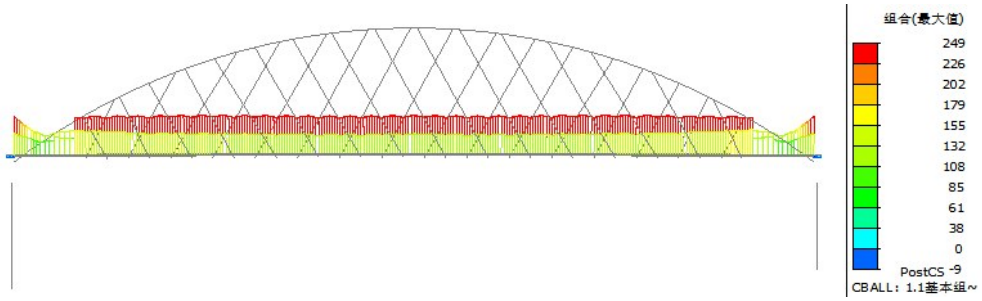

Figure 12 Total stress envelope of the main longitudinal girder under the load combination for load-carrying capacity（unit：MPa）

For the frequent load combination, the transverse crack widths of the concrete deck slab induced by longitudinal forces are shown in Table 2, all of which are less than the allowable value of 0.150 mm specified in the code. This finding indicates that the steel-concrete composite girder is suitable for network hanger tied-arch bridges and can resolve the fatigue issue encountered in the steel deck in pure steel

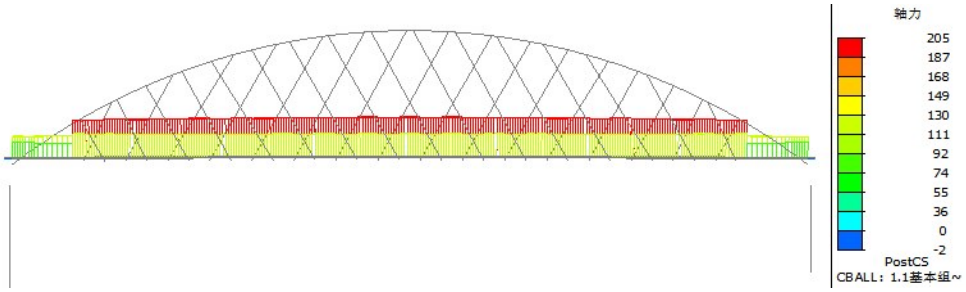

Figure 13 Axial stress envelope of the main longitudinal girder for the load combination for load-carrying capacity（unit：MPa）

Table 1 Stresses at typical locations of the main longitudinal girder for the most unfavorable load combination for load-carrying capacity

Location	Total stress (MPa)	Axial stress (MPa)	Bending stress (MPa)	Proportion of axial stress	Proportion of bending stress
Region without hangers near the arch springing point	160	114	46	71%	29%
Hanger region near the arch springing point	235	195	40	83%	17%
Hanger region at midspan	245	205	40	84%	16%

girders.

(2) Arch Rib Analysis

For the most unfavorable load combination for load-carrying capacity, the total

Table 2 Transverse crack widths of the concrete deck slab induced by longitudinal forces for the frequent load combination

Location	Stress from the first system (MPa)		Stress from the second system (MPa)		Axial force (kN/m)	Bending moment (kN·m/m)	Reinforcement stress (MPa)	Crack width (mm)
	Top fiber	Bottom fiber	Top fiber	Bottom fiber				
Midspan of the middle panel	3.10	3.20	-3.05	2.99	798	35	125	0.142
Cross-girder position of the middle panel	3.10	3.20	1.18	-1.67	755	-16	120	0.134
Midspan of the edge panel	3.10	3.10	-2.82	2.48	762	30	115	0.130
Cross-girder position of the edge panel	3.10	3.10	2.08	-2.88	702	-28	133	0.148

Tensile stress is positive and compressive stress is negative in the table.

https://doi.org/10.59238/j.pt.XXXX.XX.001

stress envelope and the axial stress envelope of the arch rib are shown in Figures 14 and 15, respectively. The maximum stress in the arch rib is 221 MPa. In accordance with the *Code for Design of Highway Steel Bridge Structures* (JTG D64—2015), after a global axial stability reduction factor of 0.66 and a local stability reduction factor of 0.96 are applied, the converted stress is 294 MPa, which is less than the allowable value of 330 MPa specified in the code. The stresses and their proportions at typical locations of the arch rib are presented in Table 3. The calculation results reveal that, except for the region without hangers near the arch springing point, the ratio of bending stress to total stress in the arch rib is less than 20% at all locations. This finding indicates that the network hanger arrangement is capable of reducing bending moments in the arch rib.

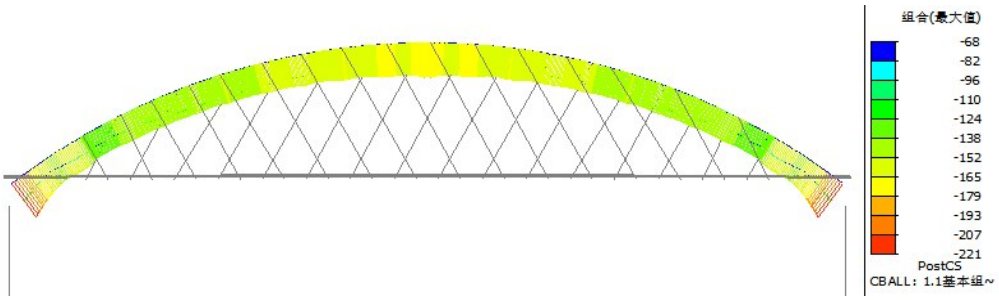

Figure 14 Total stress envelope of the arch rib for the load combination for load-carrying capacity（unit：MPa）

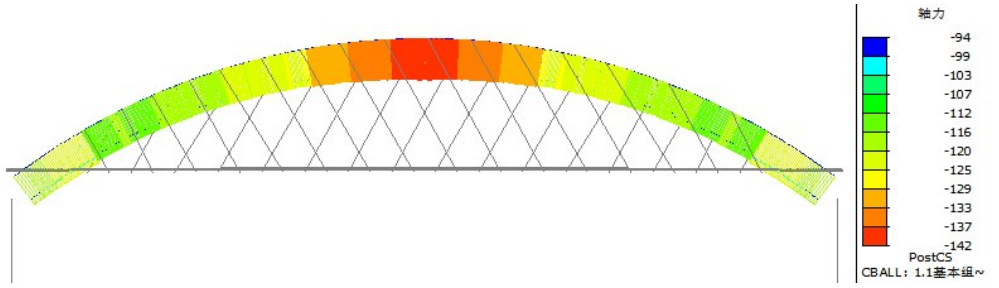

Figure 15 Axial stress envelope of the arch rib for the load combination for load-carrying capacity（unit：MPa）

Table 3 Stresses at typical locations of the arch rib for the most unfavorable load combination for load-carrying capacity

Location	Total stress (MPa)	Axial stress (MPa)	Bending stress (MPa)	Proportion of axial stress	Proportion of bending stress
Region without hangers near the arch springing point	155	120	35	77%	23%
Hanger region near the arch springing point	138	116	22	84%	16%
Hanger region at the crown	175	142	33	80%	19%

(3) Hanger Analysis

The tensile forces in the hangers for the most unfavorable load combination for load-carrying capacity are shown in Figure 16. The corresponding maximum stress in the hangers is 764 MPa (see Figure 17), which is less than the allowable value of 834 MPa specified in the code. The calculation results indicate that the distribution of the hanger tensile forces is uneven. Overall, the larger the angle between the hanger and the tangent of the arch axis is, the greater the tensile force in the hanger.

The fatigue performance of the hangers was evaluated using Calculation

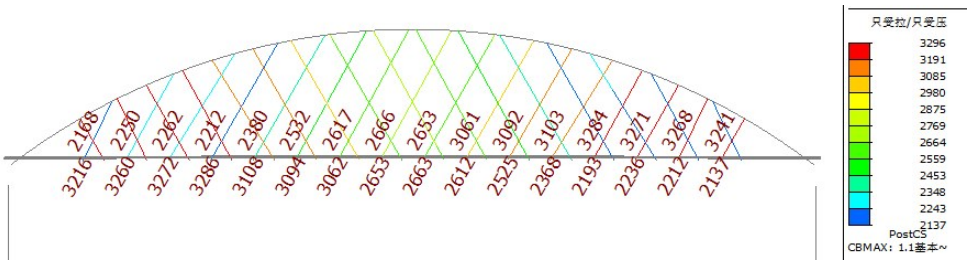

Figure 16 Envelope of tensile forces in the hangers for the load combination for load-carrying capacity（unit：kN）

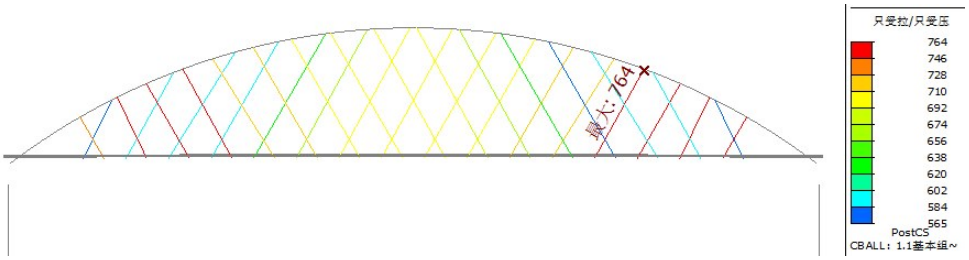

Figure 17 Envelope of stresses in the hangers for the load combination for load-carrying capacity（unit：MPa）

Model I of the *Code for Design of Highway Steel Bridge Structures* (JTG D64—2015). The corresponding maximum and minimum stresses are 39 MPa and −15 MPa, respectively, resulting in a difference in fatigue stress of 54 MPa, which is less than the allowable value of 127 MPa specified in the code. Because the main girder is a composite girder, the ratio of dead load to live load is relatively high; consequently, the difference in fatigue stress for the hangers in this bridge is not significant.

5.1.2 Local Analysis

Local analysis models of the hanger anchorage zones at the arch end and the girder end were established using finite element analysis software. The calculation results reveal that, excluding the stress concentration points, the maximum von Mises stress in the anchor plate at the arch end is 208 MPa (see Figure 18), and the maximum von Mises stress in the anchor plate at the girder end is 160 MPa (see Figure 19). Both values are less than the allowable value of 275 MPa specified in the code, indicating that the pinned anchor plate without any stiffening ribs is suitable for both the arch end and the girder end.

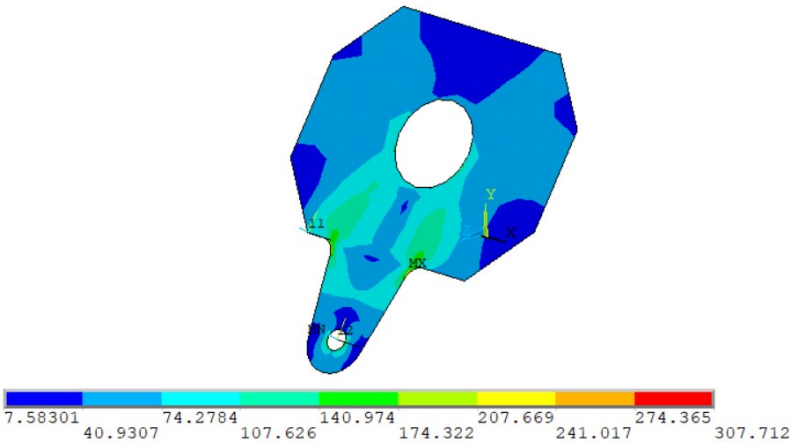

Figure 18 Von Mises stress of the hanger anchorage at the arch end（unit：MPa）

5.2 Arch Rib Stability Analysis

As a typical compression-bending member, the arch rib sustains significant axial compressive forces during service. Analysis of its global stability and verification are key aspects of structural design. Linear elastic stability analysis (eigenvalue

 https://doi.org/10.59238/j.pt.XXXX.XX.001

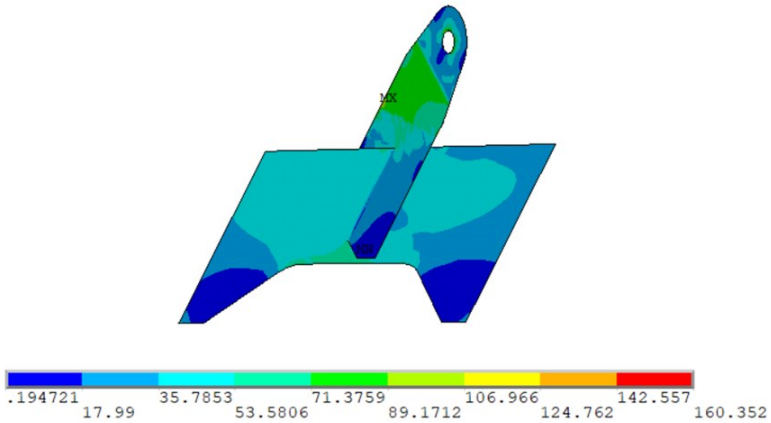

Figure 19 Von Mises stress of the hanger anchorage at the girder end（unit：MPa）

method) was performed under a combination of dead load, live load (corresponding to the maximum axial force at the crown), and wind load. The minimum out-of-plane stability safety factor of the arch rib is 4.3 (see Figure 20), and the minimum in-plane stability safety factor is 31.4 (see Figure 21). The latter is much larger than both the out-of-plane stability factor and the allowable value of 4.0 specified in the code, indicating that the network hanger tied-arch bridge has excellent in-plane stability.

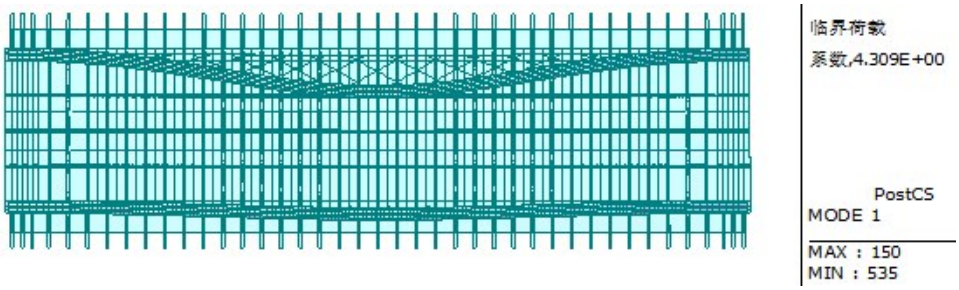

Figure 20 Out-of-plane instability mode of the arch rib

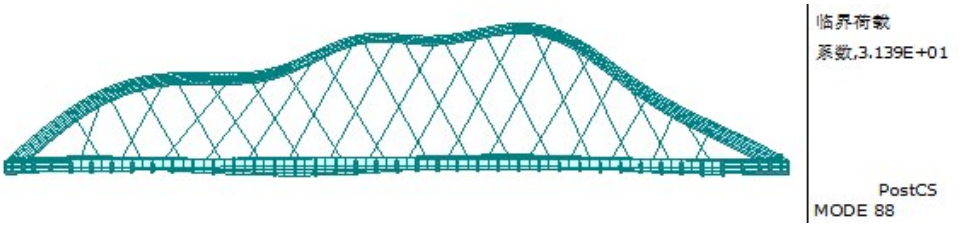

Figure 21 In-plane instability mode of the arch rib

5.3 Seismic Analysis

In accordance with the *Code for Seismic Design of Urban Bridges* (CJJ 166—2011), the main bridge of this project is classified as Grade A in terms of seismic fortification. The effects of an E1 earthquake (return period of 475 years) and an E2 earthquake (return period of 2,500 years) should be determined by seismic safety evaluation. On the basis of the ground motion acceleration time–history curves provided by the seismic safety evaluation report, a seismic isolation analysis of the main bridge was performed. For the E2 earthquake, the time–history curves of the main girder displacement in the longitudinal and transverse directions before and after isolation are shown in Figures 22 and 23, respectively.

The changes in the main girder displacement and shear force at the top of the piers before and after isolation are presented in Table 4. The results show that during the E2 earthquake, the shear pins of the bearings are sheared off. By increasing the longitudinal and transverse deformations of the main girder to dissipate

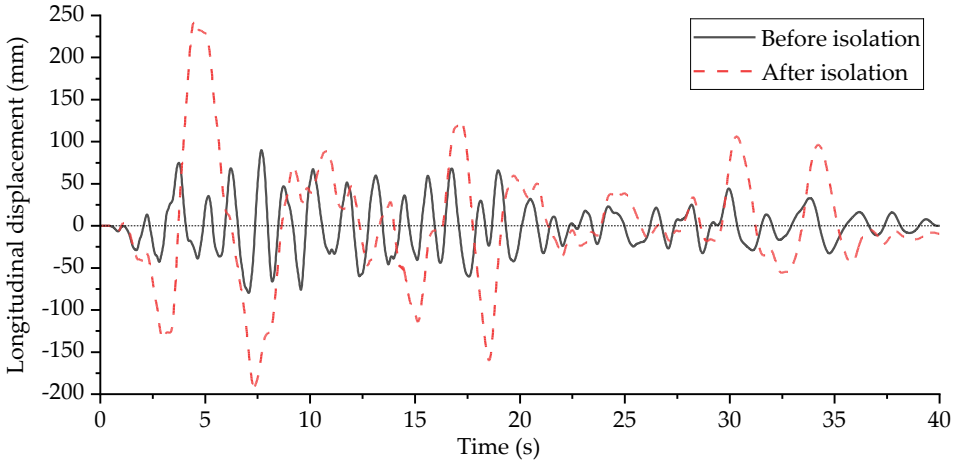

Figure 22 Time–history curves of the longitudinal displacement of the main girder before and after isolation

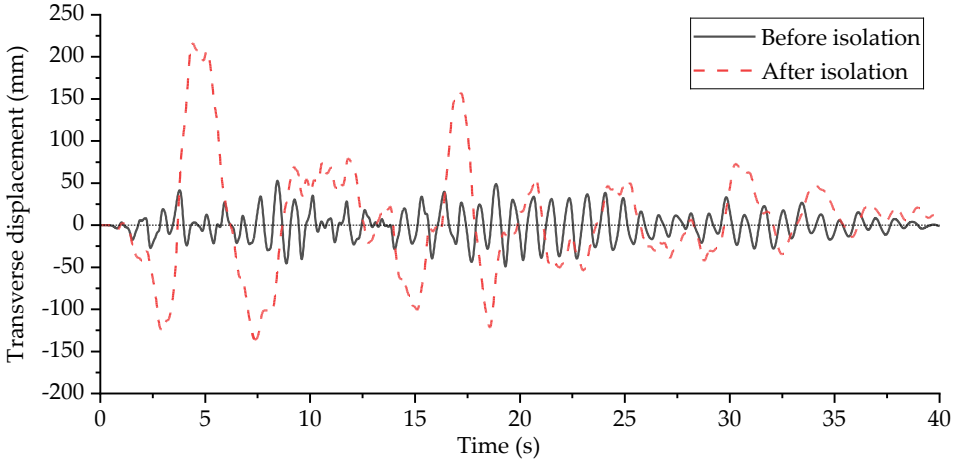

Figure 23 Time–history curves of the transverse displacement of the main girder before and after isolation

energy, the longitudinal and transverse shear forces at the top of the piers are reduced to 39% and 43% of their original values, respectively. Under these conditions, no plastic deformation occurs in the piers or pile foundations of the main bridge, and they remain in the elastic range. The seismic capacity meets the predetermined seismic fortification criteria.

Table 4 Changes in the main girder displacement and shear force at the top of the piers before and after isolation

Item	Before isolation	After isolation	Change ratio (after/before)
Max./min. longitudinal displacement of the main girder (mm)	90/–80	243/–192	270%/241%
Max./min. transverse displacement of the main girder (mm)	53/–49	216/–136	409%/277%
Longitudinal shear force at the top of the piers (kN)	18,054	6,974	39%
Transverse shear force at the top of the piers (kN)	14,844	6,450	43%

https://doi.org/10.59238/j.pt.XXXX.XX.001

6 Conclusions

Taking the 170 m span network hanger tied-arch bridge of the Guangming Road Guohe Bridge in Bozhou city as an engineering example, structural design and mechanical characteristic analysis are presented in this paper. The main conclusions are as follows:

(1) For a span of 170 m, the network hanger tied-arch bridge effectively solves the problems of traditional vertical hangers, namely, their susceptibility to slackness and insufficient stiffness under asymmetric loads. The internal force distribution of the arch rib and the main girder is optimized, significantly reducing the bending stresses and deformations. This bridge type is suitable for medium-to-large span urban bridges.

(2) The main girder is a double-box steel-concrete composite girder, which balances mechanical performance, construction efficiency, and economy while effectively avoiding the fatigue problem encountered in steel decks. For the arch rib, an octagonal steel box section without transverse bracing is adopted; together with the network hanger arrangement, it ensures structural stability while satisfying aesthetic requirements. For the hangers, pinned clevis anchorages, which are simple in terms of their construction and convenient for installation and tensioning and are well suited to the inclined arrangement of network hangers, are adopted. The substructure involves friction pendulum seismic isolation bearings with shear pins, which significantly reduce the seismic response and meet the Grade A seismic fortification requirements for Zone VII.

(3) The design and analysis results for this bridge verify the technical feasibility and economic rationality of the 170 m span network hanger tied-arch bridge. They serve as a reference for scheme selection, structural design, and mechanical analysis of similar medium-to-large span wide urban bridges.

Dongwei Luo

M.E., Senior Engineer. He Graduated from Tongji University in 2013.
Research Direction：Mainly Research on Bridge Design.

Email: 425756691@qq.com

Conflict of Interest: The authors declare that there is no conflict of interest regarding the publication of this paper.

Data Availability Statement: Data Availability**Statement:** The data that support the findings of this study are available from the corresponding author upon reasonable request.

References

1. Zhang D.; Zhou W.; Luo D.; Sun H.; Shao C. Design of 208 m-Span Network Tied-Arch Bridge of Wusong River Project. *Bridge Construction* **2025**, 55, 134-140, doi:10.20051/j.issn.1003-4722.2025.03.018.(in Chinese)
2. Shao, C. Modern Arch Bridge; China Communications Press: Beijing, 2021.
3. Shao, C. *Cable supported composite bridges*; China Communications Press: Beijing, 2017.
4. Liu Z.; Lu Z. Comparative Study on the Tied- Arch Bridges with Vertical and Inclined Hangers. *China Civil Engineering Journal* **2000**, 33, 63-67, doi:10.3321/j.issn:1000-131X.2000.05.011.(in Chinese)
5. Lin Y.; He C.; Ren S.; Lu Y. Network Tied Arch Bridge —— An Economical and Pretty Bridge Type. *Structural Engineers* **2006**, 22, 1-4, doi:10.3969/j.issn.1005-0159.2006.05.001.(in Chinese)

6. Wang Y.; Liu K.; Xiu J.; Hu Q. Design of Long-Span Network Arch Bridge with Hangers in Mountainous Areas and Analysis of Key Parameter Influences. *Highway* **2021**, 66, 124-127.(in Chinese)
7. Zhang D.; Chen L.; Zhang C.; Chang F. Overall Design of Jinli Bridge in Quanzhou. *World Bridges* **2025**, 53, 8-14, doi: 10.20052/j.issn.1671-7767.2025.02.002.(in Chinese)
8. Chen C.; Wu X.; Liu X.; Zhu Y. Overall Design of a Basket-Handle Arch Bridge with Steel Box Arch Ribs of Large Inclination Angle. *World Bridges* **2024**, 52, 13-18, doi:10.20052/j.issn.1671-7767.2024.01.003.(in Chinese)
9. Chen W.; Yuan W.; Yang H. Application of the Cable-sliding Friction Aseismic Bearing in a Tied-arch Bridge. *Structural Engineers* **2013**, 29, 84-90, doi:10.3969/j.issn.1005-0159.2013.05.014.(in Chinese) AUTHOR BIOGRAPHIES